Gamow-Teller Strengths in ^{76}Ge, ^{82}Se, ^{90}Zr, and ^{92}Zr from the Deformed Quasi-particle RPA (DQRPA)

Eunja Ha* and Myung-Ki Cheoun †

Department of Physics, Soongsil University, Seoul 156-743, Korea

(Dated: December 21, 2012)

We developed the deformed quasi-particle random phase approximation (DQRPA) to describe various properties of deformed nuclei and applied to the evaluation of the Gamow-Teller (GT) transition strength distributions which data can be extracted from the charge exchange reactions (CEXR). Our calculations started with the single-particle states calculated by the deformed axially symmetric Woods-Saxon potential. Pairing correlations of nucleons, neutron-neutron and proton-proton as well as neutron-proton pairing correlations, are explicitly taken into account at the deformed Bardeen Cooper Schriffer (BCS) theory leading to the quasi-particle concept. The ground state correlations and the two-particle and two-hole mixing states are included in the deformed QRPA. In this work, we use a realistic two-body interaction given by the Brueckner G-matrix based on the Bonn potential to reduce the ambiguity on the nucleon-nucleon interactions inside nuclei. We applied our formalism to the GT transition strengths for ^{76}Ge, ^{82}Se, ^{90}Zr, and ^{92}Zr, and compared to available experimental data. The GT strength distributions turn out to be sensitive on the deformation parameter. We suggest most probable deformation parameters for the nuclei by adjusting GT strength distributions to the experimental data and the Ikeda sum rule, which sum rule is usually thought to be satisfied more or less even under the one-body current approximation without introducing the quenching factor, if high-lying excited states are properly taken into account as in our approach. Most of the experimental GT strength data of the nuclei, in particular, on the high-lying excited states beyond one nucleon threshold are confirmed in our DQRPA by the deformation parameter.

---

* ejha@ssu.ac.kr

† cheoun@ssu.ac.kr

I.   INTRODUCTION

In the core collapsing supernovae (SNe), medium and heavy elements are believed to be produced by the rapid and slow successive neutron capture reaction, dubbed as r-process and s-process, respectively. In these processes, many unstable neutron-rich nuclei are produced iteratively and decay to more stable nuclei at their turning points in the nuclear chart. These r- and s-processes play vital roles of understanding the nuclear abundances in the cosmos [1].

Since most of the nuclei produced in the processes are thought to be more or less deformed, we need to explicitly consider effects by the deformation in the nuclear structure and their reactions in the network calculations of the processes. One interesting process related to the deformed nuclei may be the rapid proton process (p-process), which is thought to be occurred on the binary star system composed of a neutron star and a companion star, usually white dwarf. Because of the strong gravitation on the neutron star surface, one expects hydrogen rich mass flow from the companion star. Since the high density and low temperature on the neutron star crust makes electrons degenerated, beta decays are usually Pauli blocked by the degeneration, which gives rise to the pycno-reactions [2]. It means that neutron rich nuclei may become stable nuclei, while unstable nuclei may become stable in this situation.

Up to now, main conventional approach to understand the nuclear structure is based on the spherical symmetry. In order to describe neutron-rich nuclei and their relevant nuclear reactions occurred in the nuclear processes, one needs to develop theoretical formalism including explicitly the deformation [3, 4]. Ref. [3] exploited the Nilsson basis to the deformed quasi-particle random phase approximation (DQRPA). But the two-body interaction was derived from the effective separable force. The realistic two-body interaction derived from the realistic force is firstly exploited at Ref. [4] only with neutron-neutron (nn) and proton-proton (pp) pairing interactions which have only isospin T = 1 and J = 0 interaction. But, to properly describe the deformed nuclei, the T= 0 and J = 1 pairing should be also taken into account because it is intimately related to the deformation by the J = 1 pairing.

In this work, we extend our previous QRPA based on the spherical symmetry [5] to the DQRPA. The spherical QRPA has been exploited as a useful framework for describing the

2

nuclear reactions sensitive on the nuclear structure of medium-heavy and heavy nuclei [6], where, as the mass number increases, the application of the shell model may have actual limits because of tremendous increase of configuration mixing due to the deformation. This paper is organized as follows. In Sec. II, we introduce detailed formalism for the DQRPA and the Gamow-Teller (GT) strength. Numerical results and related discussions are presented at Sec. III. Summary and conclusions are addressed at Sec. IV.

II.   FORMALISM

A.   Total Hamiltonian

We start from the following nuclear Hamiltonian

$$H = H_0 + H_{\text{int}} \, , \tag{1}$$

$$H_0 = \sum_{\alpha \rho_\alpha \alpha'} \epsilon_{\alpha \rho_\alpha \alpha'} c^\dagger_{\alpha \rho_\alpha \alpha'} c_{\alpha \rho_\alpha \alpha'} \qquad (\alpha' = p, n) \, ,$$

$$H_{\text{int}} = \sum_{\alpha \beta \gamma \delta \rho_\alpha \rho_\beta \rho_\gamma \rho_\delta, \ \alpha' \beta' \gamma' \delta'} V_{\alpha \rho_\alpha \alpha' \beta \rho_\beta \beta' \gamma \rho_\gamma \gamma' \delta \rho_\delta \delta'} c^\dagger_{\alpha \rho_\alpha \alpha'} c^\dagger_{\beta \rho_\beta \beta'} c_{\delta \rho_\delta \delta'} c_{\gamma \rho_\gamma \gamma'},$$

where the interaction matrix V is the anti-symmetrized interaction with the Baranger Hamiltonian [7] in which two $\frac{-1}{2}$ factors, from J and T coupling, are included, so that the H_{int} in Eq. (1) is equivalent to the usual $H_{\text{int}} = \frac{1}{4} \sum_{\alpha \beta \gamma \delta \rho_\alpha \rho_\beta \rho_\gamma \rho_\delta, \ \alpha' \beta' \gamma' \delta'} \tilde{V}_{\alpha \rho_\alpha \alpha' \beta \rho_\beta \beta' \gamma \rho_\gamma \gamma' \delta \rho_\delta \delta'} c^\dagger_{\alpha \rho_\alpha \alpha'} c^\dagger_{\beta \rho_\beta \beta'} c_{\delta \rho_\delta \delta'} c_{\gamma \rho_\gamma \gamma'}$. The Greek letters denote proton or neutron single particle states with the projection Ω of the total angular momentum on the nuclear symmetry axis and the parity π. The projection Ω is treated as the only good quantum number in the deformed basis. The ρ_α ($\rho_\alpha = \pm 1$) is the sign of the angular momentum projection Ω of the α state. The isospin of particles is denoted as a Greek letter with prime, while the isospin of quasi-particles is expressed as a Greek letter with double prime as shown later.

Therefore, the operator $c^\dagger_{\alpha \rho_\alpha \alpha'}$ ($c_{\alpha \rho_\alpha \alpha'}$) in Eq.(1) stands for the usual creation (destruction) operator of the real particle in the state of $\alpha \rho_\alpha$ with the angular momentum projection Ω_α and an isospin α', and $c_{\bar{\alpha} \rho_\alpha \alpha'} (= (-1)^{j_a + m_\alpha} c_{-\alpha \rho_\alpha \alpha'})$ is the time reversed operator of $c_{\alpha \rho_\alpha \alpha'}$. Namely our intrinsic states are twofold-degenerate, $i.e.$ Ω_α state and its time-reversed state $-\Omega_\alpha$. $\epsilon_{\alpha \rho_\alpha \alpha'}$ means the single particle state energies.

In cylindrical coordinates, eigenfunctions of a s.p. state and its time-reversed state in deformed Woods-Saxon potential are expressed as follows

$$|\alpha \rho_\alpha = +1> = \sum_{Nn_z} [b^{(+)}_{Nn_z\Omega_\alpha} |N, n_z, \Lambda_\alpha, \Omega_\alpha = \Lambda_\alpha + 1/2 > \tag{2}$$
$$+b^{(-)}_{Nn_z\Omega_\alpha} |N, n_z, \Lambda_\alpha + 1, \Omega_\alpha = \Lambda_\alpha + 1 - 1/2 >],$$
$$|\alpha \rho_\alpha = -1> = \sum_{Nn_z} [b^{(+)}_{Nn_z\Omega_\alpha} |N, n_z, -\Lambda_\alpha, \Omega_\alpha = -\Lambda_\alpha - 1/2 >$$
$$-b^{(-)}_{Nn_z\Omega_\alpha} |N, n_z, -\Lambda_\alpha - 1, \Omega_\alpha = -\Lambda_\alpha - 1 + 1/2 >],$$

where $N = n_\perp + n_z$ ($n_\perp = 2n_\rho + \Lambda$) is a major shell number, and n_z and n_ρ are numbers of nodes on the deformed harmonic oscillator wave functions in z and ρ direction, respectively. Λ is the projection of the orbital angular momentum onto the nuclear symmetric axis z. The coefficients $b^{(+)}_{Nn_z\Omega}$ and $b^{(-)}_{Nn_z\Omega}$ are obtained by the eigenvalue equation of the total Hamiltonian in the Nilsson basis. The 2nd terms in Eg. (2) have the same projection Ω_α value as the 1st term, but retain another orbital angular momentum because of a flipped spin. Particle model spaces we used depend on the nuclei as shown later on. Single particle spectrum obtained by the deformed Woods Saxon potential is sensitive on the deformation parameter β_2 defined as

$$R(\theta) = R_0(1 + \beta_2 Y_{20}(\theta)) , \tag{3}$$

where $R_0 = 1.2A^{1/3}$fm for the sharp-cut radius R_0 [8] and Y_{20} is spherical harmonics. The customary parameter $\epsilon = 3(\omega_\perp - \omega_3)/(2\omega_\perp + \omega_3)$ used in the deformed harmonic oscillator is related to as $\beta_2 \approx (2/3)\sqrt{4\pi/5}\,\epsilon$ at the leading order. We transform the Hamiltonian represented by real particles in Eq. (1) to the quasi-particle representation through the following Hartree Fock Bogoliubob (HFB) transformation,

$$a^\dagger_{\alpha\alpha''} = \sum_{\beta\beta'} (u_{\alpha\alpha''\beta\beta'} c^\dagger_{\beta\beta'} + v_{\alpha\alpha''\beta\beta'} c_{\bar\beta\beta'}), \ a_{\bar\alpha\alpha''} = \sum_{\beta\beta'} (u^*_{\bar\alpha\alpha''\bar\beta\beta'} c_{\bar\beta\beta'} + v_{\bar\alpha\alpha''\bar\beta\beta'} c^\dagger_{\beta\beta'}). \tag{4}$$

The Hamiltonian, then, can be expressed in terms of the quasi-particles as follows

$$H' = H'_0 + \sum_{\alpha\alpha''} E_{\alpha\alpha''} a^\dagger_{\alpha\alpha''} a_{\alpha\alpha''} + H_{qp.int} . \tag{5}$$

Using the transformation of Eq. (4), finally we obtain the following HFB equation

$$
\begin{pmatrix}
\epsilon_p - \lambda_p & 0 & \Delta_{p\bar{p}} & \Delta_{p\bar{n}} \\
0 & \epsilon_n - \lambda_n & \Delta_{n\bar{p}} & \Delta_{n\bar{n}} \\
\Delta_{p\bar{p}} & \Delta_{p\bar{n}} & -\epsilon_p + \lambda_p & 0 \\
\Delta_{n\bar{p}} & \Delta_{n\bar{n}} & 0 & -\epsilon_n + \lambda_n
\end{pmatrix}_\alpha
\begin{pmatrix}
u_{\alpha''p} \\ u_{\alpha''n} \\ v_{\alpha''p} \\ v_{\alpha''n}
\end{pmatrix}_\alpha
= E_{\alpha\alpha''}
\begin{pmatrix}
u_{\alpha''p} \\ u_{\alpha''n} \\ v_{\alpha''p} \\ v_{\alpha''n}
\end{pmatrix}_\alpha ,
\qquad (6)
$$

where $E_{\alpha\alpha''}$ is the energy of a quasi-particle with the isospin quantum number α'' in the state α. If we neglect Δ_{np}, this equation reduces to the standard Deformed BCS (DBCS) equation.

B. Spherical and deformed wave functions for a single particle state

Since various mathematical theorems regarding quantum numbers may not be easily used in the deformed basis, it is more convenient to play in the spherical basis. In addition, we exploit the G-matrix based on the Bonn potential in order to pin down plausible ambiguities on the nucleon-nucleon interaction inside a deformed nucleus. Since the G-matrix is calculated on the spherical basis, we need to represent the G-matrix in terms of the deformed basis. Here we present as to how to transform deformed wave functions to spherical wave functions.

The deformed harmonic oscillator wave function, $|Nn_z\Lambda_\alpha\Omega_\alpha(=\Lambda_\alpha+\Sigma)> = |Nn_z\Lambda_\alpha>|\Sigma>$ in Eq. (2) can be expanded in terms of the spherical harmonic oscillator wave function $|N_0l\Lambda>|\Sigma>$ as follows

$$
|Nn_z\Lambda_\alpha>\ |\Sigma> = \sum_{N_0=N,N\pm2,N\pm4,\dots}\ \sum_{l=N_0,N_0-2,N_0-4,\dots} A_{Nn_z\Lambda}^{N_0l,\ n_r=\frac{N_0-l}{2}} |N_0l\Lambda_\alpha>\ |\Sigma>, \quad (7)
$$

$$
|N_0l\Lambda_\alpha>\ |\Sigma> = \sum_j C_{l\Lambda_\alpha\frac{1}{2}\Sigma}^{j\Omega_\alpha}|N_0lj\ \Omega_\alpha>.
$$

Here the spatial overlap integral $A_{Nn_z\Lambda}^{N_0l} = < N_0l\Lambda|Nn_z\Lambda >$ is calculated numerically in the spherical coordinate system. Roman letter indicates quantum numbers (n_rlj) of a nucleon state, where n_r is the radial quantum number and l is the orbital angular momentum. $C_{l\Lambda_\alpha\frac{1}{2}\Sigma}^{j\Omega_\alpha}$ is the Clebsch-Gordan coefficient of the coupling of the orbital and spin angular momenta to total angular momentum with the projection Ω_α. Therefore, the expansion can be simply written as

$$
|\alpha\Omega_\alpha> = \sum_a B_a^\alpha\ |a\Omega_\alpha>, \qquad (8)
$$

with the expansion coefficient summarized as $B_a^\alpha = \sum_{Nn_z\Sigma} C_{l\Lambda\frac{1}{2}\Sigma}^{j\Omega_\alpha} A_{Nn_z\Lambda}^{N_0 l} b_{Nn_z\Sigma}$.

The DBCS Eq. (6) is solved by using the Brueckner G-matrix calculated from the realistic Bonn CD potential for the nucleon-nucleon interaction in the following way. The pairing potentials Δ_p, Δ_n and Δ_{pn} in Eq. (6) are calculated as

$$\Delta_{\alpha p \bar{\alpha} p} = -\frac{1}{2}\frac{1}{(2a+1)^{1/2}} \sum_{J,c} g_{\text{pair}}^p (g_{\text{pair}}^n) F_{\alpha a\alpha a}^{J0} F_{\gamma c\gamma c}^{J0} G(aacc, J)(2c+1)^{1/2}(u_{1p_c}^* v_{1p_c} + u_{2p_c}^* v_{2p_c}) ,$$

(9)

where $F_{\alpha a\bar{\beta}b}^{JK'} = B_a^\alpha B_b^\beta C_{j_a\Omega_\alpha j_\beta\Omega_\beta}^{JK'}$ ($K' = \Omega_\alpha + \Omega_\beta$) is introduced for the transformation to the deformed basis of G-matrix. Here K', which is a projection number of the total angular momentum J onto the z axis, is selected $K' = 0$ at the BCS stage because we consider the pairings of the quasi-particles at α and $\bar{\alpha}$ states. $\Delta_{\alpha n \bar{\alpha} n}$ is the same as Eq. (9) with replacement of n by p. In order to renormalize the G-matrix, strength parameters, g_{pair}^p, g_{pair}^n and g_{pair}^{pn} are multiplied to the G-matrix [5] by adjusting the pairing potentials to the empirical pairing potentials, Δ_p^{emp}, Δ_n^{emp} and Δ_{pn}^{emp}. The empirical pairing potentials of protons (neutrons) and neutron-proton are evaluated by the following symmetric five term formula for the neighboring nuclei

$$\Delta_p{}^{\text{emp}} = \frac{1}{8}[M(Z+2,N) - 4M(Z+1,N) + 6M(Z,N) \tag{10}$$
$$-4M(Z-1,N) + M(Z-2,N)] ,$$

$$\Delta_n{}^{\text{emp}} = \frac{1}{8}[M(Z,N+2) - 4M(Z,N+1) + 6M(Z,N) \tag{11}$$
$$-4M(Z,N-1) + M(Z,N-2)] ,$$

$$\Delta_{pn}{}^{\text{emp}} = \pm\frac{1}{4}\{2[M(Z,N+1) + M(Z,N-1) + M(Z-1,N) + M(Z+1,N)] \tag{12}$$
$$-[M(Z+1,N+1) + M(Z-1,N+1) + M(Z-1,N-1) + M(Z+1,N-1)]$$
$$-4M(Z,N)\} ,$$

where $+(-)$ stands for even(odd) mass nuclei. As for masses in Eqs. (10) $\sim$ (12), we use empirical masses. For the neutron-rich nuclei far from the stability region, the masses are still unknown. We, thus, are going to use the values from the extrapolation or the values derived from the liquid-drop model, $\Delta \approx 12A^{-1/2}$MeV. More exact mass measurement of the exotic nuclei from the penning trap [9, 10] are greatly helpful for these empirical parameters.

C. Description of an excited state by the DQRPA

We take the ground state of a target even-even nucleus as the DBCS vacuum for a quasi-particle. In the following, we show how to generate an excited state in a deformed compound nucleus. Since the deformed nuclei have two different frames, the laboratory and the intrinsic frame, we need to consider the relationship of the two frames. The GT excited state in the intrinsic frame of even-even nuclei, which is described by operating a phonon operator to the BCS vacuum $\mathcal{Q}_{m,K}^\dagger |QRPA>$, can be transformed to the wave function in the laboratory frame by using the Wigner function $\mathcal{D}_{MK}^1(\phi, \theta, \psi)$ as follows

$$|1M(K), m> = \sqrt{\frac{3}{8\pi^2}}[\mathcal{D}_{M-K}^1(\phi, \theta, \psi)\mathcal{Q}_{m,K}^\dagger |QRPA> \quad \text{(for } K = 0), \tag{13}$$

$$|1M(K), m> = \sqrt{\frac{3}{16\pi^2}}[\mathcal{D}_{MK}^1(\phi, \theta, \psi)\mathcal{Q}_{m,K}^\dagger$$
$$+(-1)^{1+K}\mathcal{D}_{M-K}^1(\phi, \theta, \psi)\mathcal{Q}_{m,-K}^\dagger |QRPA> \quad \text{(for } K = \pm1),$$

where $M(K)$ is a projection of the total angular momentum onto the z (the nuclear symmetry) axis. Of course, the K is accepted as only a good quantum number in deformed nuclei. The QRPA phonon creation operator $\mathcal{Q}_{m,K}^\dagger$ acting on the ground state is given as

$$\mathcal{Q}_{m,K}^\dagger = \sum_{\alpha\alpha''\beta\beta''} [X_{(\alpha\alpha''\beta\beta''K)}^m A^\dagger(\alpha\alpha''\beta\beta''K) - Y_{(\alpha\alpha''\beta\beta''K)}^m \tilde{A}(\alpha\alpha''\beta\beta''K)]. \tag{14}$$

with pairing creation and annihilation operators comprising two quasi-particles defined as

$$A^\dagger(\alpha\alpha''\beta\beta''K) = a_{\alpha\alpha''}^\dagger a_{\bar{\beta}\beta''}^\dagger, \quad \tilde{A}(\alpha\alpha''\beta\beta''K) = a_{\beta\beta''}a_{\bar{\alpha}\alpha''}, \tag{15}$$

where bar denotes a time-reversal state for a given state. The quasi-particle pairs in two-particle states, α and $\bar{\beta}$, are chosen by the selection rules $\Omega_\alpha - \Omega_\beta = K$ and $\pi_\alpha\pi_\beta = 1$.

Two-body wave functions in deformed basis are calculated from the spherical basis as follows

$$|\alpha\bar{\beta}> = \sum_{abJ} F_{\alpha a\beta b}^{JK}|ab, JK>, \tag{16}$$

where 2-body wave function in the spherical basis is given as $|ab, JK> = \sum_J C_{j_a\Omega_a j_b\Omega_b}^{JK}|a\Omega_a> |b\Omega_b>$, and the transformation coefficient is calculated as $F_{\alpha a\beta b}^{JK} = B_a^\alpha B_b^\beta(-1)^{j_\beta-\Omega_\beta} C_{j_a\Omega_\alpha j_\beta-\Omega_\beta}^{JK}$ which has a phase factor $(-1)^{j_\beta-\Omega_\beta}$ arising from the time-reversed states $\bar{\beta}$. B_a^α is defined below Eq.(8).

Our QRPA equation in deformed basis leads to the following form.

$$
\left(
\begin{array}{cccccc}
A^{1111}_{\alpha\beta\gamma\delta}(K) & A^{1122}_{\alpha\beta\gamma\delta}(K) & A^{1112}_{\alpha\beta\gamma\delta}(K) & B^{1111}_{\alpha\beta\gamma\delta}(K) & B^{1122}_{\alpha\beta\gamma\delta}(K) & B^{1112}_{\alpha\beta\gamma\delta}(K) \\
A^{2211}_{\alpha\beta\gamma\delta}(K) & A^{2222}_{\alpha\beta\gamma\delta}(K) & A^{2212}_{\alpha\beta\gamma\delta}(K) & B^{2211}_{\alpha\beta\gamma\delta}(K) & B^{2222}_{\alpha\beta\gamma\delta}(K) & B^{2212}_{\alpha\beta\gamma\delta}(K) \\
A^{1211}_{\alpha\beta\gamma\delta}(K) & A^{1222}_{\alpha\beta\gamma\delta}(K) & A^{1212}_{\alpha\beta\gamma\delta}(K) & B^{1211}_{\alpha\beta\gamma\delta}(K) & B^{1222}_{\alpha\beta\gamma\delta}(K) & B^{1212}_{\alpha\beta\gamma\delta}(K) \\
& & & & & \\
-B^{1111}_{\alpha\beta\gamma\delta}(K) & -B^{1122}_{\alpha\beta\gamma\delta}(K) & -B^{1112}_{\alpha\beta\gamma\delta}(K) & -A^{1111}_{\alpha\beta\gamma\delta}(K) & -A^{1122}_{\alpha\beta\gamma\delta}(K) & -A^{1112}_{\alpha\beta\gamma\delta}(K) \\
-B^{2211}_{\alpha\beta\gamma\delta}(K) & -B^{2222}_{\alpha\beta\gamma\delta}(K) & -B^{2212}_{\alpha\beta\gamma\delta}(K) & -A^{2211}_{\alpha\beta\gamma\delta}(K) & -A^{2222}_{\alpha\beta\gamma\delta}(K) & -A^{2212}_{\alpha\beta\gamma\delta}(K) \\
-B^{1211}_{\alpha\beta\gamma\delta}(K) & -B^{1222}_{\alpha\beta\gamma\delta}(K) & -B^{1212}_{\alpha\beta\gamma\delta}(K) & -A^{1211}_{\alpha\beta\gamma\delta}(K) & -A^{1222}_{\alpha\beta\gamma\delta}(K) & -A^{1212}_{\alpha\beta\gamma\delta}(K)
\end{array}
\right) \tag{17}
$$

$$
\times
\left(
\begin{array}{c}
\tilde{X}^{m}_{(\gamma 1\delta 1)K} \\
\tilde{X}^{m}_{(\gamma 2\delta 2)K} \\
\tilde{X}^{m}_{(\gamma 1\delta 2)K} \\
\\
\tilde{Y}^{m}_{(\gamma 1\delta 1)K} \\
\tilde{Y}^{m}_{(\gamma 2\delta 2)K} \\
\tilde{Y}^{m}_{(\gamma 1\delta 2)K}
\end{array}
\right)
= \hbar\Omega^{m}_{K}
\left(
\begin{array}{c}
\tilde{X}^{m}_{(\alpha 1\beta 1)K} \\
\tilde{X}^{m}_{(\alpha 2\beta 2)K} \\
\tilde{X}^{m}_{(\alpha 1\beta 2)K} \\
\\
\tilde{Y}^{m}_{(\alpha 1\beta 1)K} \\
\tilde{Y}^{m}_{(\alpha 2\beta 2)K} \\
\tilde{Y}^{m}_{(\alpha 1\beta 2)K}
\end{array}
\right),
$$

where 1 and 2 denote the isospin quantum numbers of protons and neutrons. The amplitudes $X_{\alpha\alpha''\beta\beta''}$ and $Y_{\alpha\alpha''\beta\beta''}$, which stand for forward and backward going amplitudes from state $\alpha\alpha''$ to $\beta\beta''$, are related to $\tilde{X}_{\alpha\alpha''\beta\beta''} = \sqrt{2}\sigma_{\alpha\alpha''\beta\beta''}X_{\alpha\alpha''\beta\beta''}$ and $\tilde{Y}_{\alpha\alpha''\beta\beta''} = \sqrt{2}\sigma_{\alpha\alpha''\beta\beta''}Y_{\alpha\alpha''\beta\beta''}$. $\sigma_{\alpha\alpha''\beta\beta''} = 1$ if $\alpha = \beta$ and $\alpha'' = \beta''$, otherwise $\sigma_{\alpha\alpha''\beta\beta''} = \sqrt{2}$ [5]. The A and B matrices are given by

$$
\begin{aligned}
A^{\alpha''\beta'',\,\gamma''\delta''}_{\alpha\bar\beta,\,\gamma\bar\delta}(K) =\quad & (E_{\alpha\alpha''} + E_{\beta\beta''})\delta_{\alpha\gamma}\delta_{\alpha''\gamma''}\delta_{\bar\beta\bar\delta}\delta_{\beta''\delta''} - \sigma_{\alpha\alpha''\bar\beta\beta''}\sigma_{\gamma\gamma''\bar\delta\delta''} \\
& \times [g_{pp}(u_{\alpha\alpha''}u_{\bar\beta\beta''}u_{\gamma\gamma''}u_{\delta\delta''} + v_{\alpha\alpha''}v_{\bar\beta\beta''}v_{\gamma\gamma''}v_{\delta\delta''})\,V^{K}_{\alpha\bar\beta,\,\gamma\bar\delta} \\
& + g_{ph}(u_{\alpha\alpha''}v_{\bar\beta\beta''}u_{\gamma\gamma''}v_{\delta\delta''} + v_{\alpha\alpha''}u_{\bar\beta\beta''}v_{\gamma\gamma''}u_{\delta\delta''})\,V^{K}_{\alpha\delta,\,\gamma\beta} \\
& + g_{ph}(u_{\alpha\alpha''}v_{\bar\beta\beta''}v_{\gamma\gamma''}u_{\delta\delta''} + v_{\alpha\alpha''}u_{\bar\beta\beta''}u_{\gamma\gamma''}v_{\delta\delta''})\,V^{K}_{\alpha\gamma,\,\delta\beta}],
\end{aligned}
\tag{18}
$$

$$
\begin{aligned}
B^{\alpha''\beta'',\,\gamma''\delta''}_{\alpha\bar\beta,\,\gamma\bar\delta}(K) = -\ & \sigma_{\alpha\alpha''\bar\beta\beta''}\sigma_{\gamma\gamma''\bar\delta\delta''} \\
& \times [-g_{pp}(u_{\alpha\alpha''}u_{\bar\beta\beta''}v_{\gamma\gamma''}v_{\delta\delta''} + v_{\alpha\alpha''}v_{\bar\beta\beta''}u_{\gamma\gamma''}u_{\delta\delta''})\,V^{K}_{\alpha\bar\beta,\,\gamma\bar\delta} \\
& + g_{ph}(u_{\alpha\alpha''}v_{\bar\beta\beta''}v_{\gamma\gamma''}u_{\delta\delta''} + v_{\alpha\alpha''}u_{\bar\beta\beta''}u_{\gamma\gamma''}v_{\delta\delta''})\,V^{K}_{\alpha\delta,\,\gamma\beta} \\
& + g_{ph}(u_{\alpha\alpha''}v_{\bar\beta\beta''}u_{\gamma\gamma''}v_{\delta\delta''} + v_{\alpha\alpha''}u_{\bar\beta\beta''}v_{\gamma\gamma''}u_{\delta\delta''})\,V^{K}_{\alpha\gamma,\,\delta\beta}],
\end{aligned}
\tag{19}
$$

8

$$V_{\alpha\bar{\beta},\ \gamma\bar{\delta}}^{K} = \sum_{J}\sum_{abcd} F_{\alpha a\bar{\beta} b}^{JK} F_{\gamma c\bar{\delta} d}^{JK} G(abcd,\ J)\ , \tag{20}$$

$$V_{\alpha\bar{\delta},\ \gamma\bar{\beta}}^{K} = \sum_{J}\sum_{abcd} F_{\alpha a\bar{\delta} d}^{JK'} F_{\gamma c\bar{\beta} b}^{JK'} G(adcb,\ J)\ ,$$

$$V_{\alpha\gamma,\ \delta\beta}^{K} = \sum_{J}\sum_{abcd} F_{\alpha a\gamma c}^{JK} F_{\beta b\delta d}^{JK} G(acdb,\ J).$$

where $F_{\alpha a\bar{\beta} b}^{JK'} = B_a^{\alpha}\ B_b^{\beta}\ C_{j_\alpha\Omega_\alpha j_\beta\Omega_\beta}^{JK'}$ with non-zero $K' = \Omega_\alpha + \Omega_\beta$, and u and v coefficients are determined from deformed HFB calculation with the pairing strength $g_{\text{pair}}^n, g_{\text{pair}}^p$ and g_{pair}^{np} adjusted to the empirical pairing gaps Δ_{nn}, Δ_{pp} and Δ_{np}, respectively. $E_{\alpha\alpha''}$ indicates the quasi-particle energy of the state α with the quasi-particle isospin α''. The $G(F)$ matrices are two body particle - particle (hole) matrix elements obtained as solutions of the Bethe - Goldstone equation from the Bonn potential [11]. If we do not consider the np pairing correlations, the A and B matrices can be expressed in the following simple form, which is the same as the those of Saleh [4],

$$\begin{aligned} A_{\alpha\bar{\beta},\ \gamma\bar{\delta}}^{pn,\ p'n'}(K) = \quad & (E_{\alpha p} + E_{\bar{\beta} n})\delta_{\alpha\gamma}\delta_{pp'}\delta_{\bar{\beta}\bar{\delta}}\delta_{nn'} \tag{21} \\ & - 2\left[g_{pp}(u_{\alpha p}u_{\bar{\beta} n}u_{\gamma p'}u_{\bar{\delta} n'} + v_{\alpha p}v_{\bar{\beta} n}v_{\gamma p'}v_{\bar{\delta} n'})\ V_{\alpha\bar{\beta},\ \gamma\bar{\delta}}^{K}\right. \\ & + g_{ph}(u_{\alpha p}v_{\bar{\beta} n}u_{\gamma p'}v_{\bar{\delta} n'} + v_{\alpha p}u_{\bar{\beta} n}v_{\gamma p'}u_{\bar{\delta} n'})\ V_{\alpha\bar{\delta},\ \gamma\bar{\beta}}^{K}\Big], \end{aligned}$$

$$\begin{aligned} B_{\alpha\bar{\beta},\ \gamma\bar{\delta}}^{pn,\ p'n'}(K) = \ & - 2\left[-g_{pp}(u_{\alpha p}u_{\bar{\beta} n}v_{\gamma p'}v_{\bar{\delta} n'} + v_{\alpha p}v_{\bar{\beta} n}u_{\gamma p'}u_{\bar{\delta} n'})\ V_{\alpha\bar{\beta},\ \gamma\bar{\delta}}^{K}\right. \tag{22} \\ & + g_{ph}(u_{\alpha p}v_{\bar{\beta} n}v_{\gamma p'}u_{\bar{\delta} n'} + v_{\alpha p}u_{\bar{\beta} n}u_{\gamma p'}v_{\bar{\delta} n'})\ V_{\alpha\bar{\delta},\ \gamma\bar{\beta}}^{K}\Big]\ . \end{aligned}$$

D.   Description of Gamow-Teller Transition

The $\beta^{\pm}$ decay operator, $\hat{\beta}_{1\mu}^{\pm}$, is defined in the intrinsic frame as

$$\hat{\beta}_{1\mu}^{-} = \sum_{\alpha_p\rho_\alpha\beta_n\rho_\beta} <\alpha_p\rho_\alpha|\tau^{+}\sigma_K|\beta_n\rho_\beta> c_p^{\dagger}\tilde{c}_n,\ \hat{\beta}_{1\mu}^{+} = (\hat{\beta}_{1\mu}^{-})^{\dagger} = (-)^{\mu}\hat{\beta}_{1,-\mu}^{-}, \tag{23}$$

in which the $\hat{\beta}_{1\mu}^{\pm}$ transition operators are related with those in the laboratory system $\hat{\beta}_M^{\pm}$ operator as follows

$$\hat{\beta}_M^{\pm} = \sum_{\mu} \mathcal{D}_{M\mu}^{1}(\phi, \theta, \psi)\hat{\beta}_{1\mu}^{\pm}. \tag{24}$$

The $\beta^{\pm}$ transition amplitudes from the ground state of an initial nucleus to the excited state, the one phonon state in a final nucleus, are expressed by

$$< 1(K), m|\hat{\beta}_K^-| \, QRPA > \tag{25}$$

$$= \sum_{\alpha\alpha''\rho_\alpha\beta\beta''\rho_\beta} \mathcal{N}_{\alpha\alpha''\rho_\alpha\beta\beta''\rho_\beta} < \alpha\alpha''p\rho_\alpha|\sigma_K|\beta\beta''n\rho_\beta > [u_{p\alpha\alpha''}v_{n\beta\beta''}X_{\alpha\alpha''\beta\beta'',K} + v_{p\alpha\alpha''}u_{n\beta\beta''}Y_{\alpha\alpha''\beta\beta'',K}]$$

$$< 1(K), m|\hat{\beta}_K^+| \, QRPA >$$

$$= \sum_{\alpha\alpha''\rho_\alpha\beta\beta''\rho_\beta} \mathcal{N}_{\alpha\alpha''\beta\beta''} < \alpha\alpha''p\rho_\alpha|\sigma_K|\beta\beta''n\rho_\beta > [u_{p\alpha\alpha''}v_{n\beta\beta''}Y_{\alpha\alpha''\beta\beta'',K} + v_{p\alpha\alpha''}u_{n\beta\beta''}X_{\alpha\alpha''\beta\beta'',K}]$$

where $| \, QRPA >$ denotes the correlated QRPA ground state in the intrinsic frame and the nomalization factor is given as $\mathcal{N}_{\alpha\alpha''\beta\beta''}(J) = \sqrt{1 - \delta_{\alpha\beta}\delta_{\alpha''\beta''}(-1)^{J+T}}/(1 + \delta_{\alpha\beta}\delta_{\alpha''\beta''})$. The Wigner functions are disappeared by using the orthogonality of two Wigner functions from the operator and the excited state, respectively. This form is also easily reduced to the results by proton-neutron DQRPA without the np pairing

$$< 1(K), m|\hat{\beta}_K^-| \, QRPA > \tag{26}$$

$$= \sum_{\alpha_p\rho_\alpha\beta_n\rho_\beta} < \alpha_p\rho_\alpha|\tau^+\sigma_K|\beta_n\rho_\beta > \; [u_{\alpha_p}v_{\beta_n}X_{\alpha_p\beta_n,K} + v_{\alpha_p}u_{\beta_n}Y_{\alpha_p\beta_n,K}] \; ,$$

$$< 1(K), m|\hat{\beta}_K^+| \, QRPA >$$

$$= \sum_{\alpha_p\rho_\alpha\beta_n\rho_\beta} < \alpha_p\rho_\alpha|\tau^+\sigma_K|\beta_n\rho_\beta > \; [u_{\alpha_p}v_{\beta_n}Y_{\alpha_p\beta_n,K} + v_{\alpha_p}u_{\beta_n}X_{\alpha_p\beta_n,K}].$$

Here single particle matrix elements of $\langle\alpha_p\rho_\alpha|\tau^+\sigma_K|\beta_n\rho_\beta\rangle$ can be expressed in deformed basis [3],

$$< \alpha_p\rho_\alpha|\tau^+\sigma_{K=0}|\beta_n\rho_\beta >= \delta_{\Omega_p\Omega_n}\rho_\alpha \sum_{Nn_z}[b^{(+)}_{Nn_z\Omega_p}b^{(+)}_{Nn_z\Omega_n} - b^{(-)}_{Nn_z\Omega_p}b^{(-)}_{Nn_z\Omega_n}], \tag{27}$$

$$< \alpha_p\rho_\alpha|\tau^+\sigma_{K=1}|\beta_n\rho_\beta > \quad = -\sqrt{2}\delta_{\Omega_p\Omega_n+1}\sum_{Nn_z}b^{(+)}_{Nn_z\Omega_p}b^{(-)}_{Nn_z\Omega_n} \quad (\rho_\alpha = \rho_\beta = +1) \tag{28}$$

$$= +\sqrt{2}\delta_{\Omega_p\Omega_n+1}\sum_{Nn_z}b^{(-)}_{Nn_z\Omega_p}b^{(+)}_{Nn_z\Omega_n} \quad (\rho_\alpha = \rho_\beta = -1)$$

$$= -\sqrt{2}\delta_{\Omega_p\frac{1}{2}}\delta_{\Omega_n-\frac{1}{2}}\sum_{Nn_z}b^{(+)}_{Nn_z\Omega_p}b^{(+)}_{Nn_z\Omega_n} \quad (\rho_\alpha = +1, \rho_\beta = -1),$$

$$< \alpha_p\rho_\alpha|\tau^+\sigma_{K=-1}|\beta_n\rho_\beta > \quad = \sqrt{2}\delta_{\Omega_p\Omega_n-1}\sum_{Nn_z}b^{(-)}_{Nn_z\Omega_p}b^{(+)}_{Nn_z\Omega_n} \quad (\rho_\alpha = \rho_\beta = +1) \tag{29}$$

$$= -\sqrt{2}\delta_{\Omega_p\Omega_n-1}\sum_{Nn_z}b^{(+)}_{Nn_z\Omega_p}b^{(-)}_{Nn_z\Omega_n} \quad (\rho_\alpha = \rho_\beta = -1)$$

$$= +\sqrt{2}\delta_{\Omega_p-\frac{1}{2}}\delta_{\Omega_n\frac{1}{2}}\sum_{Nn_z}b^{(+)}_{Nn_z\Omega_p}b^{(+)}_{Nn_z\Omega_n} \quad (\rho_\alpha = +1, \rho_\beta = -1).$$

To compare our theoretical results to the experimental data, the GT($\mp$) strength functions and their running sums (total strengths) are calculated as

$$B_{GT}^-(m) = \sum_{K=0,\pm 1} | < 1(K), m || \hat{\beta}_K^- || \, QRPA > |^2, \tag{30}$$

$$B_{GT}^+(m) = \sum_{K=0,\pm 1} | < 1(K), m || \hat{\beta}_K^+ || \, QRPA > |^2,$$

$$S_{GT}^- = \sum_{K=0,\pm 1} \sum_m | < 1(K), m || \hat{\beta}_K^- || \, QRPA > |^2, \tag{31}$$

$$S_{GT}^+ = \sum_{K=0,\pm 1} \sum_m | < 1(K), m || \hat{\beta}_K^+ || \, QRPA > |^2.$$

E. Ikeda Sum Rule

Numerical results for total GT($\pm$) strengths, S_{GT}^- and S_{GT}^+, in Eq. (31) are investigated through the Ikeda sum-rule (ISR), which is known to be satisfied more or less independently of the constructed excited states by any nuclear models,

$$S_{GT}^- - S_{GT}^+ = 3(N - Z). \tag{32}$$

The ISR within the Deformed QRPA, denoted as ISR II, is given by

$$
\begin{aligned}
&(S_{GT}^- - S_{GT}^+)_{ISR\ II} \\
&= \sum_{K=0,\pm 1} \sum_m [\, | < 1(K), m || \hat{\beta}_K^- || \, QRPA > |^2 - | < 1(K), m || \hat{\beta}_K^+ || \, QRPA > |^2] \\
&= \sum_{\alpha_p \rho_\alpha \beta_n \rho_\beta} \sum_{K=0,\pm 1} \sum_m | < \alpha_p \rho_\alpha | \tau^+ \sigma_K | \beta_n \rho_\beta > |^2 \, (u_{\alpha_p}^2 v_{\beta_n}^2 - v_{\alpha_p}^2 u_{\beta_n}^2) [(X_{\alpha_p \beta_n, K}^m)^2 - (Y_{\alpha_p \beta_n, K}^m)^2] \,.
\end{aligned}
\tag{33}
$$

If we use the closure relation for the excited states, the ISR which we denote as ISR I is shown to be easily calculated as follows

$$
\begin{aligned}
&(S_{GT}^- - S_{GT}^+)_{ISR\ I} \\
&= \sum_{\alpha_p \rho_\alpha \beta_n \rho_\beta} \sum_{K=0,\pm 1} | < \alpha_p \Omega_p | \tau^+ \sigma_K | \beta_n \Omega_n > |^2 (v_{\beta_n}^2 - v_{\alpha_p}^2) \,.
\end{aligned}
\tag{34}
$$

Since we use the limited particle model space in deformed basis under the one-body current without the Δ excitation, the above sum rule is a bit broken, but it may be used to test our

nuclear model and their numerical calculations as shown in our numerical results. On the other hand, the ISR in spherical basis is easily shown to satisfy the ISR as follows

$$
\begin{aligned}
S_{GT}^- - S_{GT}^+ \quad &= \sum_{a_p b_n} | <a_p|\tau^+\sigma|b_n> |^2 (v_n^2 - v_p^2) \qquad (35) \\
&= \sum_{a_p b_n} (2j_a+1)(2j_b+1)\delta_{n_a n_b}\delta_{l_a l_b} \begin{Bmatrix} \frac{1}{2} & \frac{1}{2} & 1 \\ j_b & j_a & l_a \end{Bmatrix}^2 (v_n^2 - v_p^2) \\
&= 3\sum_{b_n}(2j_b+1)v_n^2 - 3\sum_{a_p}(2j_a+1)v_p^2 = 3(N-Z).
\end{aligned}
$$

III.   RESULTS

We calculated the Gamow-Teller (GT) strength, $B_{GT}^\pm$ in Eq. (30), for ^{76}Ge, ^{82}Se, ^{90}Zr, and ^{92}Zr within the DQRPA. Those nuclei are selected to represent medium-heavy nuclei which have experimental data relevant to the GT strength. The single particle states are used up to $4\hbar\omega$ for all nuclei, in the spherical limit.

Since the GT strength distributions turn out to be sensitive on the deformation parameter, β_2 in Eq.(3), we exploited various values of the deformation parameter, $|\beta_2| \leq 0.3$, as the default values. For the pairing interaction, the strength parameters g_{pair}^n and g_{pair}^p in Eq.(9), which are introduced to renormalize the finite Hilbert model particle space, are adjusted to reproduce the empirical pairing gaps through symmetric five term formula Eqs.(10)-(12) [5]. Corresponding values of the deformation parameter β_2, theoretical and empirical pairing gaps are tabulated in Table I with the ISR I and II in Eqs.(33) and (34). It is a remarkable point that theoretical ISR results are well satisfied within 15 % maximally, and nearly independent of the deformation parameter, β_2, as required in the sum rule.

The single particle state energies adopted from the deformed Woods Saxon potential naturally depends on the parameter β_2. The deformation of nuclei may be conjectured to come from macroscopic phenomena, for example, the core polarization, the high spin states and so on. Microscopic reasons may be traced to the tensor force in nucleon-nucleon interaction, which is known to account for the shell evolution according to the recent systematic shell model calculations [12, 13]. For example, T = 0, J = 1 pairing, which is associated with the $^3S_0$ tensor force, may lead to the deformation contrary to the spherical T = 1, J = 0 pairing. Therefore, the deformation parameters adopted in this work may include implicitly

and effectively such effects, because the single particle states from the deformed Wood Saxon potential show a strong dependence on the β_2 [14].

The deformation parameter β_2 may help us to conjecture the nuclear shape through the intrinsic quadrupole moment, $Q = \sqrt{16\pi/5}(3/4\pi)AR_0^2\beta_2$, where $R_0 = 1.2A^{1/3}$fm for the sharp-cut radius R_0 [15, 16]. In experimental side, the deformation parameter β_2 can be extracted from the E2 transition probability, $Q = \sqrt{16\pi B(E2)/5e^2}$. Since we do not have yet enough E2 data to be exploited in the nuclei considered here to our knowledge, we refer to theoretical results by the relativistic mean field theory (RMF) [17]. But the sign of the β_2 is sometimes still uncertain and also the coexistence of prolate and oblate shapes are also possible. In this work, such coexistence and β_4 deformation are not taken into account.

In the DQRPA stage, we took the particle-hole and particle-particle strength parameters, g_{ph} and g_{pp} in Eqs.(18)-(19) as 1.0 for for the four nuclei. Actually g_{ph} might be determined from the Gamow Teller Giant Resonance (GTGR), while fine tuning of g_{pp} are usually performed for the double beta decay [5]. In this work, we fix them because the GT strength distributions are not so sensitive on the values.

Since the nuclei considered here are expected to have large energy gaps between proton and neutron spaces, we considered only the nn and pp pairing correlation although the formalism is presented generally. For example, in the neutron-rich nuclei of importance in the r-process, the np pairing may not contribute so much. But for the p-process, the np pairing could be more important than in the neutron-rich nuclei because of the adjacent energy gaps of protons and neutrons. The calculations for the neutron-deficient nuclei in p-process are in progress by the explicit inclusion of the np pairing correlations.

In the following, we show the GT strength distribution in terms of the β_2 parameter, as a function of excited energy of parent nucleus. Therefore, experimental data, which were usually measured w.r.t. the the ground state of daughter nuclei, are presented by subtracting the empirical Q values from the measured data.

In Figs.1 and 2, we show the GT($-$) strength of ^{76}Ge as a function of the excitation energy E_{ex} w.r.t. the ground state of ^{76}Ge, whose Q value is 0.9233 MeV. The uppermost two panels are the experimental data from the ^{76}Ge(p,n)^{76}As reaction at 134.4 MeV [18], which show a strong GT state peak around 12 MeV. Fig.1 represent the calculated GT strength with prolate shapes, $\beta_2 = 0.1 \sim 0.3$, and Fig.2 is for oblate shapes, $\beta_2 = -0.1 \sim -0.35$. The GT strength distributions are widely scattered owing to deformation.

In particular, the results for $\beta_2 = 0.35$, in which the ISR I and II are almost satisfied as shown in Table 1, nicely reproduce the peak on the high-lying excited GT states around 12 MeV. Therefore, the redistribution of the GT strength by the deformation is not a simple wide scattering, but should be understood as the redistribution well matched to the high-lying excited states to be confirmed in the experiments. Our β_2 value is consistent with the prolate shape suggested by the RMF calculation, whose value was $\beta_2 = 0.157$ [17] a bit smaller than the present value.

The GT($-$) strength, B(GT$-$), on ^{82}Se is presented, in Fig.3, as a function of the excitation energy E_{ex} w.r.t. the ground state of ^{82}Se (whose Q value is 0.092 MeV) for $\beta_2 = \pm 0.1 \sim \pm 0.2$. The uppermost panel of Fig.3 is the experimental data from the ^{82}Se(p,n)^{82}Br reaction at 134.4 MeV [18]. Particularly, the strong strength on the high-lying excited GT state around 12 MeV is neatly reproduced by the $\beta_2 = 0.2$ at (c) panel. For a reference, the β_2 value from the RMF is 0.133 [17]. Our theoretical calculations address a possibility of another peak around 16 MeV.

The forward GT amplitudes $X_{\alpha\alpha''\beta\beta'',K}$ for three highest GT transition peaks at 10.74 and 11.51 MeV in (c) panel of Fig.3 are shown in Fig.4. Main transitions turn out to come from the (431 3/2) $\to$ (440 1/2) at 10.74 MeV, and (301 3/2) $\to$ (301 1/2) and (411 3/2) $\to$ (411 1/2) transition at 11.51 MeV around the Fermi surface, respectively. They are thought to result from the 2p-2h configuration mixing stemming from the deformation around the Fermi surface.

Figs.5 and 6 show the GT($\mp$) strength on ^{90}Zr as a function of the excitation energy E_{ex} w.r.t. ^{90}Zr, whose Q values for GT($\mp$) are 6.111 and 2.280 MeV, respectively. The uppermost panels (a) stand for the experimental data on GT($-$) and GT($+$) deduced from the ^{90}Zr(p,n)^{90}Nb reaction ^{90}Zr(n,p)^{90}Y at 293 MeV [19], respectively. Panels (c)$\sim$(d) are the results by the DQRPA for two different prolate and oblate β_2 values. For a reference, in panel (b), we show results by the spherical QRPA [5, 20]. The ISR I and II are almost satisfied at each β_2 value for both B(GT($\mp$)). If we recollect that the experimental GT strengths on the high-lying states beyond 30 MeV actually include the contributions by the isovector spin monopole (IVSM) [19] which are not considered in the present calculation, our spherical QRPA (SQRPA) (b) and DQRPA (c) for $\beta_2 = 0.1$ results seem to be consistent with the data.

It means that the ^{90}Zr is thought to be near to a spherical shape, $i.e.$ almost spherical.

14

But the DQRPA results by $\beta_2 = 0.1$ show peaks below $Q_{EC} = 6.111$ MeV of ^{90}Zr which are inconsistent with the data. Since our DQRPA is based on the intermediate deformation, the extension to small β_2 values may not be a proper treatment, if we understand that the angular momentum projection Ω_j may have angular momenta higher than j, and may go back to different j values in the $\beta_2 = 0$ limit. One more interesting point is that almost spherical nuclei, such as ^{90}Zr, did not show the high-lying GT(–) excited states appeared on ^{76}Ge and ^{82}Se. The high-lying states at the GT(+) transition is also neatly explained as shown at (c) in Fig.6.

Fig.7 show the GT(–) strength of ^{92}Zr as a function of the excitation energy E_{ex} w.r.t. the ground state of ^{92}Zr, whose Q value is 2.005 MeV. The uppermost panel (a) of Fig.7 represent the experimental B(GT$^-$) values extracted from ^{92}Zr(p,n)^{92}Nb reaction at 26MeV, which energy was too low to expect high-lying excited states. Excitation energies observed in this reaction are located below 9 MeV. Panels (b) is the our results for $\beta_2 = 0.1$.

IV. SUMMARY AND CONCLUSION

To describe deformed nuclei, we performed the deformed axially symmetric Woods-Saxon potential, the deformed BCS, and the deformed QRPA with realistic two-body interaction calculated by Brueckner G-matrix based on Bonn CD potential. Results of the Gamow-Teller strength, B(GT±), for ^{76}Ge, ^{82}Se, ^{90}Zr, and ^{92}Zr show that the deformation effect leads to a fragmentation of the GT strength into high-lying GT excited states, in particular, on ^{76}Ge and ^{82}Se which GT data were already measured at the charge exchange reaction experiments by the 134.4 MeV proton beam. Those states are shown to be properly explained by the deformation effects.

These high-lying excited GT states may affect seriously relevant nuclear reactions, particularly for neutrino-induced reactions, exploited in the nucleosynthesis because the emitted neutrinos from the proto-neutron star may have a high energy tail up to tens of MeV energy range. Since the experiments relate to the neutrino reaction on such a high energy would be a very challenging task in the present neutrino factories, the extraction of the high-lying GT states from charge exchange reactions could be very useful for understanding the neutrino reaction in the cosmos, if we recollect that the GT transitions are main components for the neutrino-induced reaction.

More systematic analysis of deformed nuclei by our DQRPA are under progress by including light nuclei characterized by the shell evolution or the inversion island. In the light nuclei or neutron-deficient nuclei, which may have small energy gaps between protons and neutrons and small N-Z values, the neutron-proton pairing correlations could definitely affect nuclear β^+ decays and Ikeda sum rule. Therefore GT(+) strength distribution data on the nuclei could be a stringent test of nuclear models.

Acknowledgement

References

[1] T. Hayakawa, N. Iwamoto, T. Shizuma, T. Kajino, H. Umeda, and K. Nomoto, Phys. Rev. Lett. **93**, 161102 (2004).

[2] P. Haensel and J. L. Zdunik, Nucl. Phys. (Proc. Suppl.) **B 24**, 139 (1991).

[3] F. Simkovic, L. Pacearescu, and A. Faessler, Nucl. Phys. **A 733**, 321 (2004).

[4] M. S. Yousef, V. Rodin, A. Faessler, and F. Simkovic, Phys. Rev. C **79**, 014314 (2009).

[5] M. K. Cheoun, A. Bobyk, Amand Faessler, F. Simcovic and G. Teneva, Nucl. Phys. **A 561**, 74 (1993) ; Nucl. Phys. **A 564**, 329 (1993); M. K. Cheoun, G. Teneva and Amand Faessler, Prog. Part. Nucl. Phys. **32**, 315 (1994) ; M. K. Cheoun, G. Teneva and Amand Faessler, Nucl. Phys. **A 587**, 301 (1995).

[6] Myung-Ki Cheoun, Eunja Ha, K. S. Kim, and Toshitaka Kajino, J. Phys. **G 37**, 055101 (2010).

[7] M. Baranger, Phys. Rev. **130**, 1244 (1963).

[8] P. Ring, Y. K. Gambhir, and G. A. Lalazissis, Comput. Phys. Commun. **105**, 77 (1997).

[9] K. Blaum, Phys. Rep. **425**, 1 (2006).

[10] G. Bollen *et al.*, Nuccl. Inst. and Method in Phys. Res. Sec. **A 368**, 675 (1997).

[11] K. Holinde, Phys. Rep. **68**, 121 (1981).

[12] T. Otsuka, Toshio Suzuki, Rintaro Fujimoto, Hubert Grawe, and Yoshinori Akaishi, Phys. Rev. Lett. **95**, 232502 (2005).

[13] T. Otsuka, Toshio Suzuki, Michio Honma, Yutaka Utsuno, Naofumi Tsunoda, Koshiroh Tsukiyama, and Morten Hjorth-Jensen, Phys. Rev. Lett. **104**, 012501 (2010).

[14] S. G. Nilsson and I. Ragnarsson, *Shapes and Shells in Nuclear Structure* (Cambridge University Press, Cambridge, UK, 1995)

[15] K. Hagino, N. W. Lwin, and M. Yamagami, Phys. Rev. C **74**, 017310 (2006).

[16] P. Raghavan, At. data Nucl. Data tables **42**, 189(1989).

[17] G. A. Lalazissis, S. Raman, P. Ring, At. Data and Nucl. Data tables **71**, 1-40 (1999).

[18] R. Madey, *et al.*, Phys. Rev. C **40**, 540 (1989).

[19] K. Yako, *et al.*, Phys. Lett. B **615**, 193 (2005).

[20] Myung-Ki Cheoun, Eunja Ha, Su Youn Lee, K.S. Kim, W.Y. So, Toshitaka Kajino, Phys. Rev. **C81**, 028501 (2010).

[21] S. M. Grimes, *et al.*, Phys. Rev. C **53**, 2709 (1996).

TABLE I: Deformation parameters β_2 and empirical (theoretical) pairing gap parameters $\Delta_{\text{em}}^{\text{p,n}}$ ($\Delta_{\text{th}}^{\text{p,n}}$) used in this work. The ISR in the last column denotes the Ikeda sum rules I (Eq.(34)) and II (Eq.(33)) as a percentage ratio to $3(N - Z)$. The particle-particle (particle-hole) strength parameters are exploited as $g_{\text{pp}} = 1.0$ ($g_{\text{ph}} = 1.0$) for all nuclei.

| nucleus	β_2	$\Delta_{\text{em}}^{\text{p}}$(MeV)	$\Delta_{\text{th}}^{\text{p}}$(MeV)	$\Delta_{\text{em}}^{\text{n}}$(MeV)	$\Delta_{\text{th}}^{\text{n}}$(MeV)	ISR I, II(%)
	0.1		1.575		1.538	97.04, 106.03
	0.2		1.578		1.540	96.94, 102.40
^{76}Ge	0.35	1.564	1.562	1.535	1.545	96.48, 99.54
	-0.1		1.578		1.542	97.20, 102.74
	-0.2		1.561		1.549	97.04, 109.01
	-0.3		1.566		1.562	97.34, 115.27
	0.1		1.502		1.579	96.51, 106.45
^{82}Se	0.2	1.409	1.419	1.544	1.547	95.62, 107.55
	-0.1		1.410		1.564	96.58, 104.89
	-0.2		1.568		1.549	96.57, 109.69
^{90}Zr	0.1	1.247	1.267	1.705	1.713	97.38, 107.41
	-0.1		1.269		1.714	97.88, 88.40
^{92}Zr	0.1	1.357	1.378	0.841	0.847	97.32, 98.18
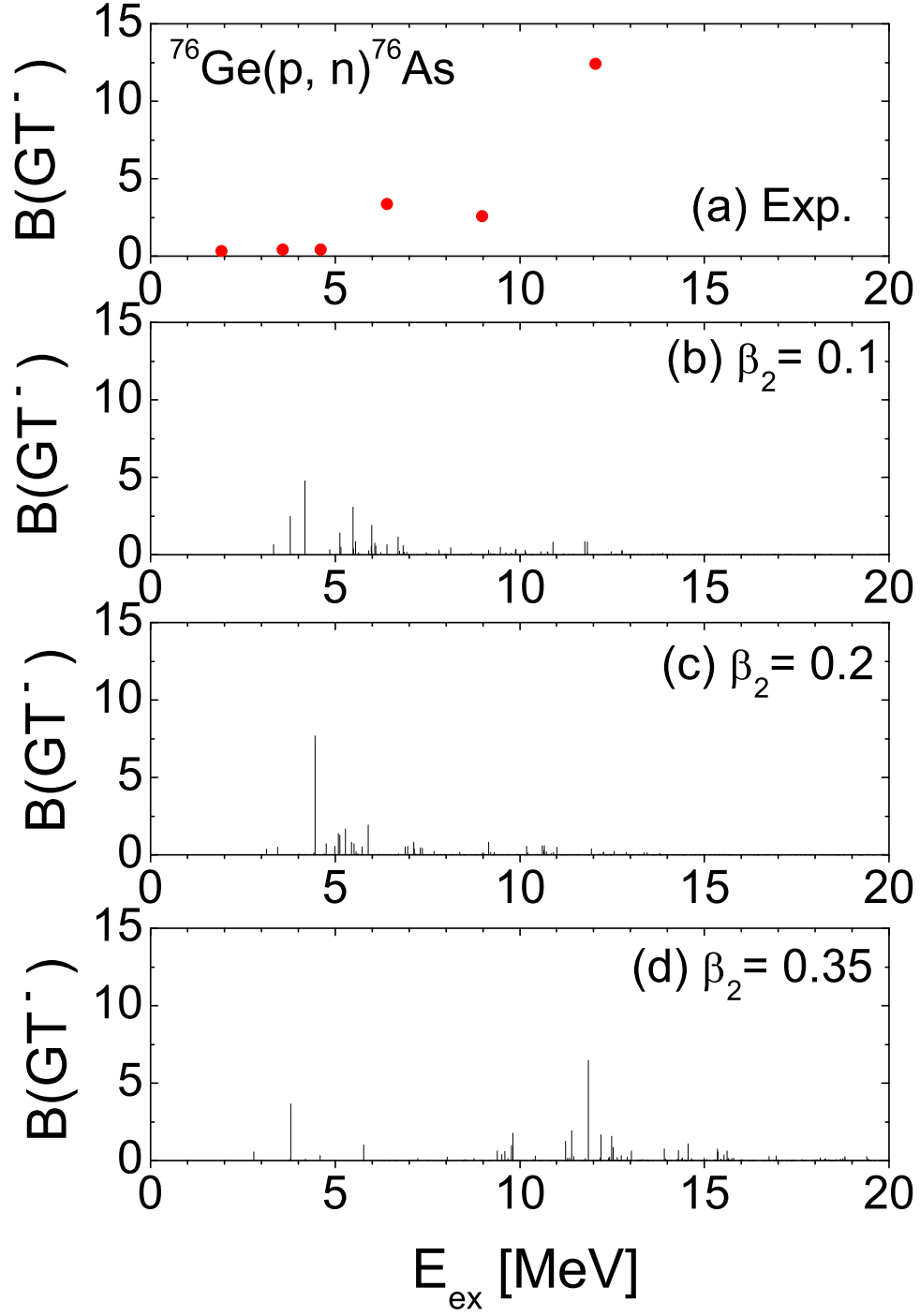
FIG. 1: (Color online) Gamow-Teller strength distributions $B(GT^-)$ on ^{76}Ge as a function of the excitation energy E_{ex} w.r.t. the ground state of ^{76}Ge. Experimental data denoted as filled (red) points in the uppermost panels are deduced from the ^{76}Ge(p,n) reaction at 134.4 MeV [18]. In each panel, we indicate $\beta_2 = 0.1 \sim 0.35$ for prolate shapes.

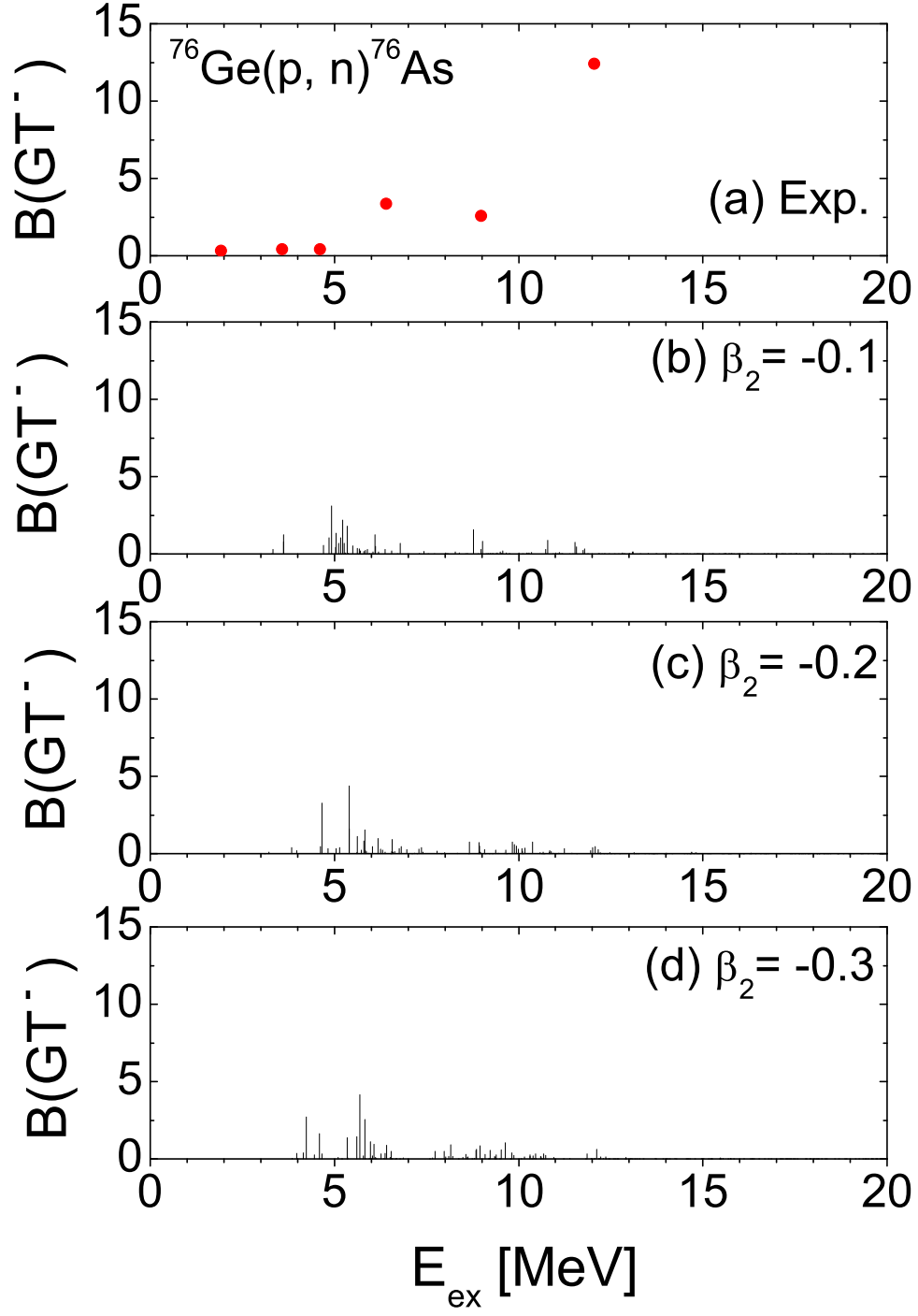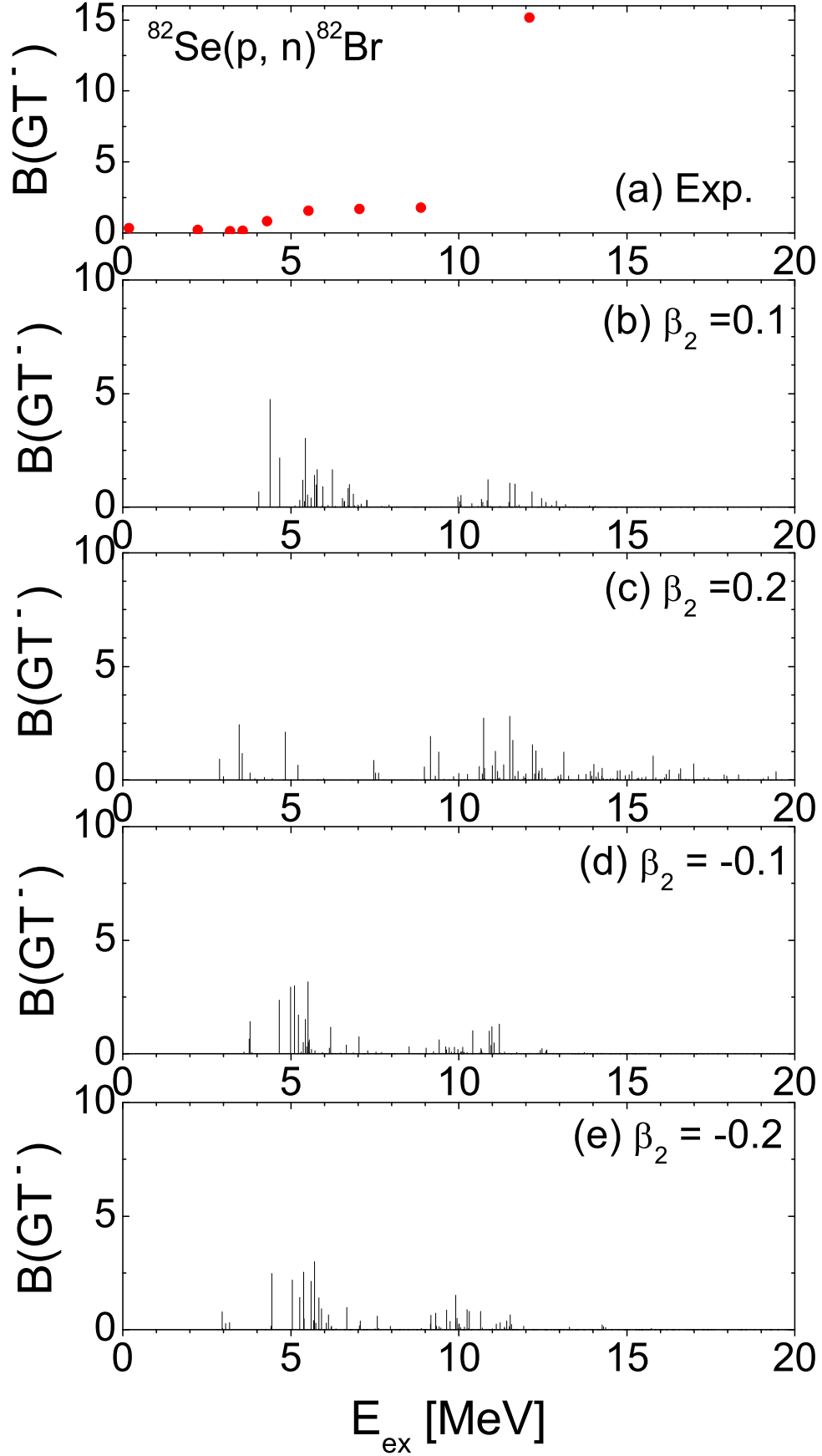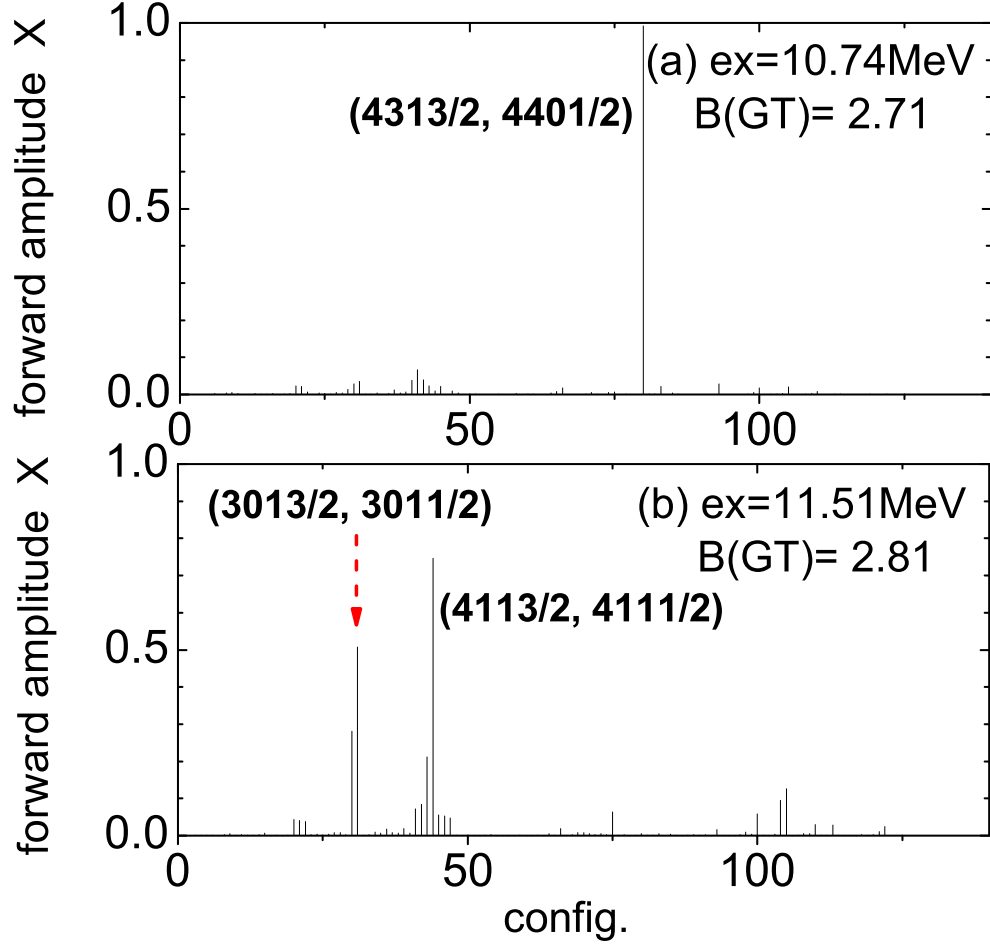FIG. 2: (Color online) The same as in Fig.1, but for oblate shapes, $\beta_2 = -0.1 \sim -0.3$.

FIG. 3: (Color online) Gamow-Teller strength distributions B(GT⁻) on ⁸²Se as a function of the excitation energy E_{ex} w.r.t. the ground state of ⁸²Se. Experimental data denoted as filled (red)

FIG. 4: Forward amplitudes X of the two highest GT strengths in (c) panel of Fig.3 at 10.74 and 11.51 MeV w.r.t. the ground state of ^{82}Se among the GT transition configuration mixing. Transition (4 3 1 3/2, 4 4 0 1/2) is the only physical component to the GT state at 10.74 MeV, and (3 0 1 3/2, 3 0 1 1/2) and (4 1 1 3/2, 4 1 1 1/2) transitions are main components for the GT state at 11.51 MeV.
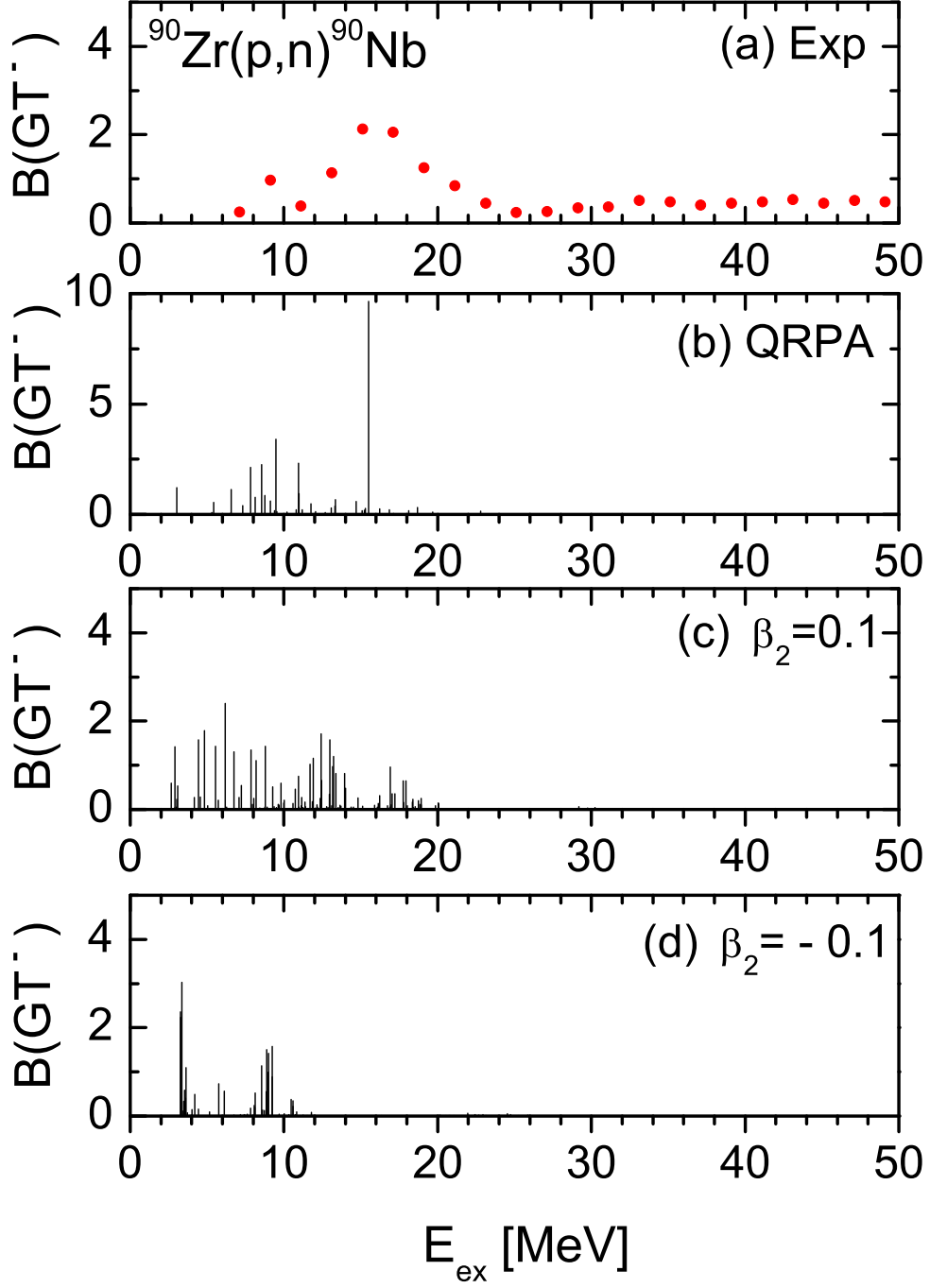
FIG. 5: (Color online) Gamow-Teller strength distributions B(GT$^-$) on ^{90}Zr as a function of the excitation energy E_{ex} w.r.t. the ground state of ^{90}Zr. Experimental data denoted as filled (red) points in the uppermost panels are deduced from the ^{90}Zr(p,n) reaction at 293 MeV [19]. In each panel, we indicate β_2.

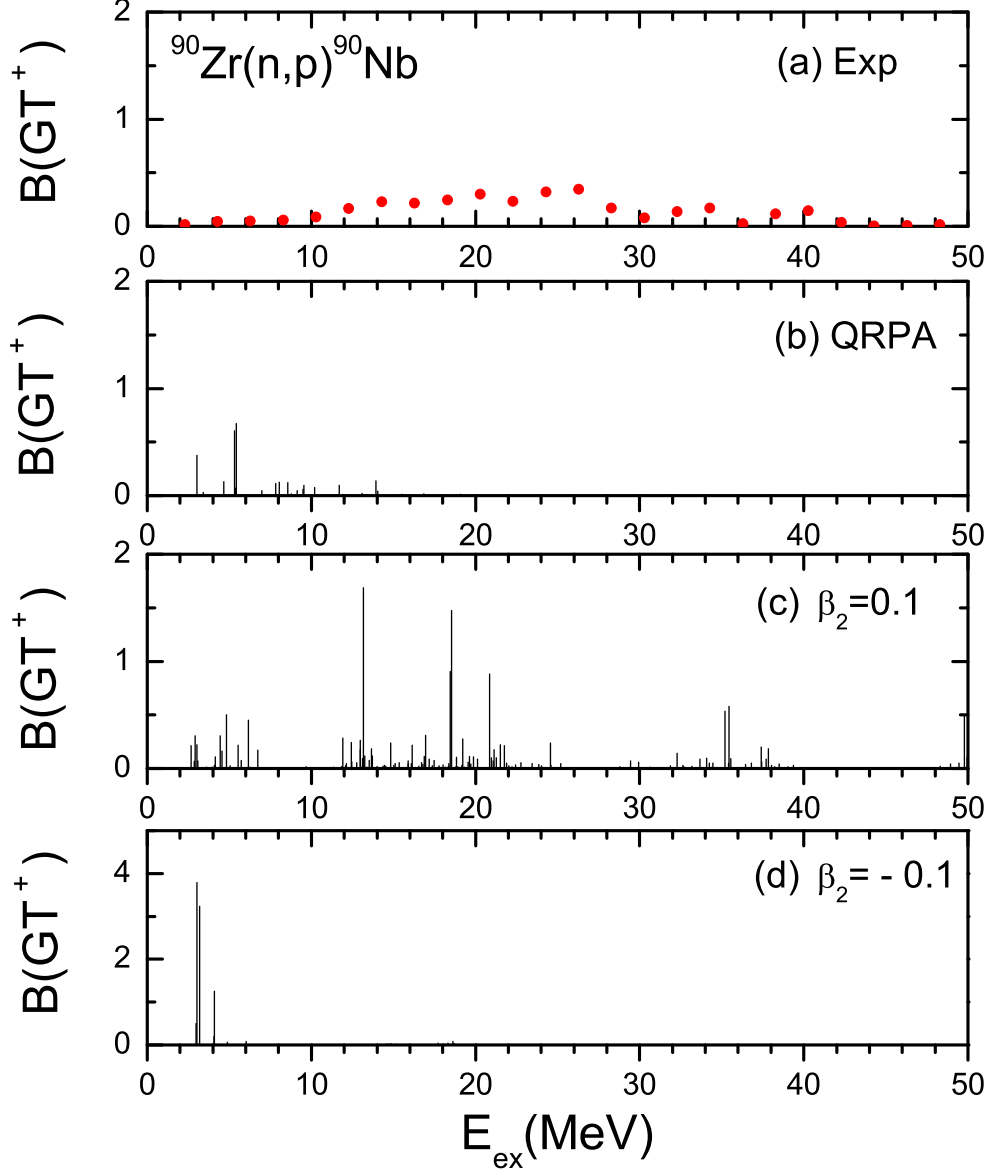FIG. 6: (Color online) Gamow-Teller strength distributions B(GT$^+$) on ^{90}Zr as a function of the excitation energy E_{ex} w.r.t. the ground state of ^{90}Zr. The filled (red) circles in the uppermost panels are deduced from the ^{90}Zr(n,p) reaction at 293 MeV [19]. In each panel, we indicate β_2.
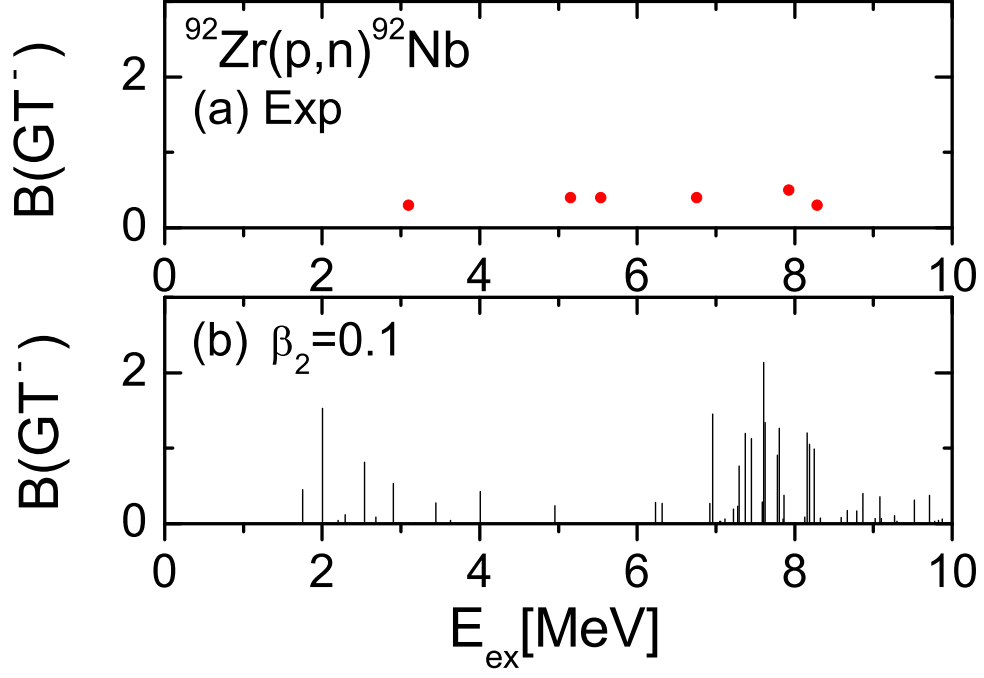
FIG. 7: (Color online) Gamow-Teller strength distributions B(GT$^-$) on ^{92}Zr as a function of the excitation energy E_{ex} w.r.t. the ground state of ^{92}Zr. Experimental data denoted as filled (red) points in the uppermost panels are deduced from the ^{92}Zr(p,n) reaction at 26 MeV [21]. In each panel, we indicate β_2.